

Theoretical Investigation of the Large Nonlinear Optical Properties of (HCN)_n Clusters with Li Atom

Wei Chen, Zhi-Ru Li,* Di Wu, Rui-Yan Li, and Chia-Chung Sun

State Key Laboratory of Theoretical and Computational Chemistry, Institute of Theoretical Chemistry, Jilin University, Jiefang Road 119, Changchun 130023, PR China

Received: May 7, 2004; In Final Form: October 21, 2004

Two new classes of (HCN)_n⋯Li and Li⋯(HCN)_n (*n* = 1, 2, 3) clusters with the electrone character characteristic are formed in theory by the metal Li atom attaching to the (HCN)_n (*n* = 1, 2, 3) clusters. Because of the interaction between the Li atom and the (HCN)_n part, the 2s valence electron of the Li atom becomes a loosely bound excess electron. Our high-level ab initio calculations show that these new clusters with the excess electron have large first hyperpolarizabilities, for example, $\beta_0 = -15\,258$ au for (HCN)⋯Li and $\beta_0 = -3401$ au for Li⋯(HCN) at the QCISD/6-311++G(3df,3pd) level (only $\beta_0 = -2.8$ au for HCN monomer²⁶). Obviously, the excess electron from the Li atom plays a crucial role in the large first hyperpolarizabilities of these clusters. The β_0 value of (HCN)_n⋯Li ($\beta_0 > 10^4$ au, from $\sigma \rightarrow \pi^*$ transition) is larger than that of Li⋯(HCN)_n ($\beta_0 > 10^3$ au, from $\sigma \rightarrow \sigma^*$ transition) for *n* = 1, 2, or 3. In addition, two interesting rules have been observed. They are that $|\beta_0|$ decreases with lengthening of the HCN chain for (HCN)_n⋯Li clusters and that $|\beta_0|$ increases as *n* increases for Li⋯(HCN)_n clusters. In this paper, we discuss two classes of clusters that are highly similar to the electrone structure model, of which the structural characteristics are that alkali metal atoms ionize to form cations and trapped electrons under the action of other polar molecules. Thus, the investigation on the large first hyperpolarizabilities of (HCN)_n⋯Li and Li⋯(HCN)_n (*n* = 1, 2, 3) may prompt one to study the unusual nonlinear optical responses of some electrines.

1. Introduction

During the past twenty years, people have expressed great interest in studying many different types of nonlinear optical (NLO) matter^{1–9} in order to design excellent NLO materials. In our previous work, it was reported that the electron-solvated cluster, (FH)₂{e}(HF), has large NLO responses (the first hyperpolarizability $\beta_0 = 8.1 \times 10^6$ au).¹⁰ The investigation shows that its large first hyperpolarizability derives from the loosely bound excess electron in (FH)₂{e}(HF).

Recently, “electrines” have interested scientists in many fields. Electrines¹¹ are novel compounds in which alkali metals ionize to form bound alkali cations and excess electrons.¹² In a recent *Science* article,^{13a} Dye considered that these excess electrons in electrines are weak-binding and, rather, occupy sites normally populated by anions such as Cl[−] and OH[−]. Matsuishi S. and co-workers^{13b} point out that chemically trapped electrons could be viewed as the smallest possible anions, and such materials could serve as strong reducing agents; from a physics standpoint, the stabilization of numerous bound electrons, or *F* centers, could provide new approaches to preparing conductive materials with magnetic or unusual optical properties. At present, magnetic, electrical, and spectroscopic studies of some electrines have been reported,^{11,14} and the photolysis and photoelectron emission of some electrines have been also studied,¹⁵ but the investigation on the NLO properties of electrines has not been reported. We consider that the excess electrons should bring some electrines large NLO responses and present our research in this paper.

The (HCN)_n⋯Li and Li⋯(HCN)_n species studied in this paper are two prototypes of the electrines. In these models, the

metal Li atom is attached to (HCN)_n (*n* = 1, 2, 3) clusters to form two new classes of alkali metal–molecule clusters. Obviously, under the action of the (HCN)_n cluster, the Li atom ionizes and resembles Li⁺ with a Rydberg-like excess electron,¹⁶ as shown in Figure 2 (the HOMO plots). It shows that two classes of clusters have more electrone-like characteristics. Recently, the dipole-bound anion [e⋯(HCN)_n] has been vigorously studied.^{17,18} For this species, the excess electron is bound because of the dipole potential of the (HCN)_n cluster. Obviously, the excess electron in the (HCN)_n⋯Li and Li⋯(HCN)_n species should be more stable than one in the [e⋯(HCN)_n] species, which is an advantage to the experimental study.

In the present work, we investigate the electrical properties of (HCN)_n⋯Li and Li⋯(HCN)_n (*n* = 1, 2, 3) in detail, especially the static first hyperpolarizability. Our goal is to reveal that new alkali metal–molecule clusters with electrone characteristics have large NLO responses, and we further deduce that some electrines should have large NLO properties.

The $|\beta_0|$ values of (HCN)_n⋯Li are quite large (15 682 au for *n* = 1, 14 159 au for *n* = 2, and 13 119 au for *n* = 3). And, the $|\beta_0|$ values of Li⋯(HCN)_n (3385 au for *n* = 1, 4790 au for *n* = 2, and 5206 au for *n* = 3) are smaller than those of (HCN)_n⋯Li but still much larger than the β_0 values of some metal–ligand crystals. For instance, the β_0 value of *trans*-1-ferrocenyl-2-(4-nitrophenyl)ethylene is only 30.8×10^{-30} esu (~ 3195 au).¹⁹ Undoubtedly, the loosely bound excess electron plays a crucial role in the large NLO properties of (HCN)_n⋯Li and Li⋯(HCN)_n. Our work may prompt one to find a new potential NLO material, electrines, with the development of the room-temperature stable electrines.^{11,13,20,21}

* E-mail: lzh@mail.jlu.edu.cn.

2. Methods of Calculation

The energy of a molecular system in the weak and homogeneous electric field can be written as²²

$$E = E^0 - \mu_\alpha F_\alpha - \frac{1}{2} \alpha_{\alpha\beta} F_\alpha F_\beta - \frac{1}{6} \beta_{\alpha\beta\gamma} F_\alpha F_\beta F_\gamma \quad (1)$$

where E^0 is the molecular energy without the applied electrostatic field, and F_α is a component of the strength on the α direction of the applied electrostatic field; μ_α , $\alpha_{\alpha\beta}$, and $\beta_{\alpha\beta\gamma}$ may be called components of the dipole, polarizability, and first hyperpolarizability tensor, respectively. $(\text{HCN})_n \cdots \text{Li}$ and $\text{Li} \cdots (\text{HCN})_n$ are typical linear structure clusters. For the linear structure cluster, there are one independent component (μ_z) for the dipole moment, two independent components (α_{xx} and α_{zz}) for the dipole polarizability, and two independent components (β_{xxz} and β_{zzz}) for the first hyperpolarizability (with z as the cluster axis).

The total dipole moment is defined by

$$\mu_0 = \mu_z \quad (2)$$

The mean and the anisotropy of the dipole polarizability are defined by

$$\bar{\alpha} = \frac{1}{3} (2\alpha_{xx} + \alpha_{zz}) \quad (3)$$

$$\Delta\alpha = \alpha_{zz} - \alpha_{xx} \quad (4)$$

The first hyperpolarizability is defined as

$$\beta_0 = \beta_z = \frac{3}{5} (2\beta_{xxz} + \beta_{zzz}) \quad (5)$$

The geometries of $(\text{HCN})_n \cdots \text{Li}$ and $\text{Li} \cdots (\text{HCN})_n$ ($n = 1, 2, 3$) with real frequencies are optimized at the MP2/6-311++G(2df,2p) level. The calculations of the vertical ionization energies (VIEs) employ the CCSD(T)/6-311++G(2df,2p) method. Basis set effects on the electrical properties are investigated with 6-311++G(2d,2p), 6-311++G(2df,2p), 6-311++G(3df,3pd), 6-311++G(3d2f,3pd), 6-311++G(3df,3pd)+D1, and 6-311++G(3df,3pd)+D2 basis sets. For the latter two basis sets, two sets of diffuse basis functions (D1 and D2) are added on the Li atom, respectively, which are D1 = 0.0037sp + 0.001 85sp + 0.000 925sp + 0.025d + 0.0125d (3s3p2d) and D2 = 0.0037sp + 0.001 85sp + 0.000 925sp + 0.000 462 5sp + 0.025d + 0.0125d + 0.006 25d (4s4p3d). In all calculations, the $\langle S^2 \rangle$ values in MP2 wave functions are 0.7505 for $(\text{HCN})_n \cdots \text{Li}$ and $\text{Li} \cdots (\text{HCN})_n$ ($n = 1, 2, 3$). We employ the Hartree–Fock theory (HF), the second-order perturbation theory (MP2), the fourth-order perturbation theory using single, double, and quadruple substitutions (MP4(SDQ)), coupled-cluster theory with both single and double substitutions (CCSD), and quadratic configuration interaction using single and double substitution (QCISD) to study the electron correlation effects on the polarizability and first hyperpolarizability.

A widely used alternative procedure is the counterpoise (CP) method²³ to scale the contribution of the Li atom to the polarizability and first hyperpolarizability in $(\text{HCN})_n \cdots \text{Li}$ and $\text{Li} \cdots (\text{HCN})_n$ ($n = 1, 2, 3$) systems. We could define the contribution of Li as

$$\bar{\alpha}(\text{Li}) = \bar{\alpha}(\text{ALi}) - \bar{\alpha}(\text{A}) \quad (6)$$

$$\bar{\beta}(\text{Li}) = \bar{\beta}(\text{ALi}) - \bar{\beta}(\text{A}) \quad (7)$$

where A stands for $(\text{HCN})_n$ ($n = 1, 2$, and 3) and $\bar{\alpha}(\text{A})$ for the mean dipole polarizability of the A moiety in the presence of the ghost orbitals of the Li atom. $\bar{\beta}(\text{A})$ is defined in the same way.

All of the calculations in this work are carried out using the GAUSSIAN 03 package.²⁴ Atomic units are used throughout this paper.

3. Results and Discussions

3.1. Geometrical Characteristics of $(\text{HCN})_n \cdots \text{Li}$ and $\text{Li} \cdots (\text{HCN})_n$ ($n = 1, 2, 3$). The optimized structures of $(\text{HCN})_n \cdots \text{Li}$ and $\text{Li} \cdots (\text{HCN})_n$ ($n = 1, 2, 3$) clusters are presented in Figure 1 and Table 1. Obviously, the $\text{N} \cdots \text{Li}$ distances (2.095 Å for $n = 1$, 2.065 Å for $n = 2$, and 2.059 Å for $n = 3$) are shorter than the $\text{Li} \cdots \text{H}$ distances (4.178 Å for $n = 1$, 3.969 Å for $n = 2$, and 3.912 Å for $n = 3$). For $(\text{HCN})_n \cdots \text{Li}$, the 2s electron of the Li atom is pushed out by the N atom and localized near the Li atom at the opposite side of the $(\text{HCN})_n$ part (see Figure 1a). For $\text{Li} \cdots (\text{HCN})_n$, the 2s electron is pulled to the H atom and localized between the H atom and the Li atom (see Figure 1b). Thus, the 2s electron of the Li atom becomes the excess electron. In Figure 2, for every structure, an excess electron occupies the dispersive orbital (HOMO) and acts as the loosely bound state. The calculations show that the HOMO for these clusters mainly consists of 3s and 4s orbitals of the Li atom, which has been proven to be the Rydberg state orbital by natural population analysis. Thus, the excess electron in the HOMO presents the Rydberg-like state, named the Rydberg-like excess electron by Iwata S. et al.¹⁶

By contrast with the $[\text{e} \cdots (\text{HCN})_n]$, the VIEs of $(\text{HCN})_n \cdots \text{Li}$ or $\text{Li} \cdots (\text{HCN})_n$ clusters are much larger than the vertical detachment energies of the $[\text{e} \cdots (\text{HCN})_n]$ ¹⁷ (see Table 1). The reason is that there is a great difference in the origin of the excess electron between $(\text{HCN})_n \cdots \text{Li}$ or $\text{Li} \cdots (\text{HCN})_n$ and $[\text{e} \cdots (\text{HCN})_n]$. For $[\text{e} \cdots (\text{HCN})_n]$, the excess electrons are bound because of the dipole potential of the neutral clusters, while the excess electrons of $(\text{HCN})_n \cdots \text{Li}$ and $\text{Li} \cdots (\text{HCN})_n$ clusters come from the Li atom by interacting with the $(\text{HCN})_n$ part. Clearly, the excess electron in $(\text{HCN})_n \cdots \text{Li}$ or $\text{Li} \cdots (\text{HCN})_n$ clusters is bound more tightly in comparison with $[\text{e} \cdots (\text{HCN})_n]$. Although this may reduce the NLO properties of $(\text{HCN})_n \cdots \text{Li}$ and $\text{Li} \cdots (\text{HCN})_n$, its high stability is an advantage to the experimental study.

3.2. Computational Details. The choice of suitable applied electric field, basis set and theoretical level is important to calculate the NLO properties of the species with an excess electron. Hence, we select the suitable computational methods for the NLO properties of $(\text{HCN})_n \cdots \text{Li}$ or $\text{Li} \cdots (\text{HCN})_n$ ($n = 1, 2, 3$) by first investigating the $(\text{HCN})_n \cdots \text{Li}$ and $\text{Li} \cdots (\text{HCN})_n$ clusters.

A. Suitable Applied Electric Field (AEF). The calculated results of polarizabilities and first hyperpolarizabilities rely on an applied electric field (AEF). The strong AEF has a large effect on the static first hyperpolarizability. To show the intrinsic characteristics of the molecular clusters accurately, the calculation of their NLO properties should use a weak AEF.

We have tested the effects of the AEFs carefully. Two components of the first hyperpolarizability (β_x and β_z) are calculated at the MP2 level of theory with the 6-311++G(3df,3pd) and 6-311++G(3df,3pd)+D2 basis sets (D2 = 0.0037sp + 0.001 85sp + 0.000 925sp + 0.000 4625sp + 0.025d + 0.0125d + 0.006 25d is added on the Li atom) in a series of AEFs from 0.0004 au to 0.0040 au. Data of the AEF dependence are displayed in Table 2.

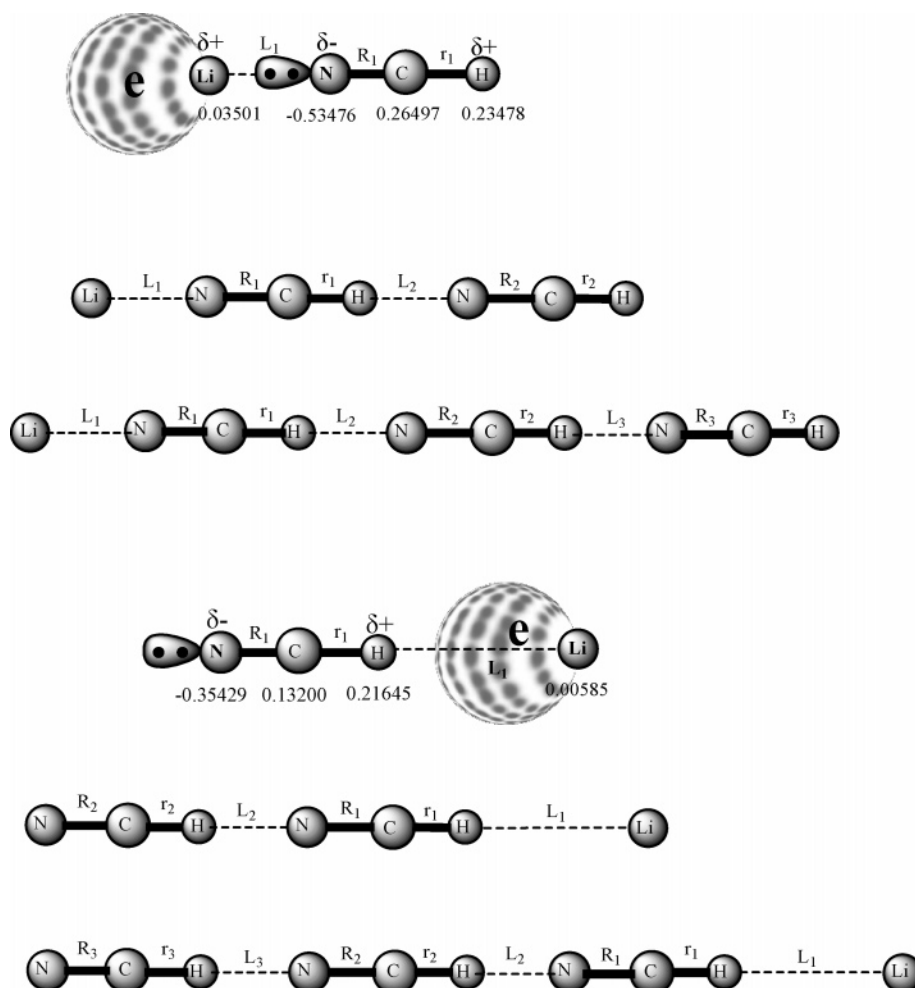


Figure 1. Internal coordinates for (HCN)_n...Li and Li...(HCN)_n (*n* = 1, 2, 3) and NBO charge distribution for *n* = 1.

TABLE 1: Optimized Geometric Parameters of (HCN)_n...Li and Li...(HCN)_n (*n* = 1, 2, 3) and VIE^a

system	<i>i</i>	<i>r_i^b</i>	<i>R_i^c</i>	<i>L_i^d</i>	VIE
(HCN)•••Li	1	1.0695	1.1648	2.0952	4.15
(HCN) ₂ •••Li	1	1.0780	1.1663	2.0651	3.89
	2	1.0690	1.1693	2.1415	
(HCN) ₃ •••Li	1	1.0804	1.1665	2.0586	3.79
	2	1.0764	1.1695	2.0927	
	3	1.0690	1.1694	2.1816	
Li•••(HCN)	1	1.0686	1.1714	4.1784	5.66
Li•••(HCN) ₂	1	1.0699	1.1697	3.9688	5.85
	2	1.0739	1.1717	2.5245	
Li•••(HCN) ₃	1	1.0704	1.1694	3.9122	5.95
	2	1.0756	1.1702	2.2004	
	3	1.0752	1.1718	2.2184	
[e•••(HCN) _n] ¹⁷	2				512 (cm ⁻¹) ^e
	3				1099 (cm ⁻¹)

^a Distances in Å and VIE in eV. ^b The C–H bond length. ^c The C–N bond length. ^d Intermolecular distances (N–Li or H–Li). ^e 1 cm⁻¹ = 1.239 81 × 10⁻⁴ eV.

The results of Table 2 show that, for (HCN)•••Li and Li•••(HCN), both β_X and β_Z change little with the increase of AEF at the MP2/6-311++G(3df,3pd) level. However, at the MP2/6-311++G(3df,3pd)+D2 level, the β_X and β_Z values of two clusters have great changes with the increase of AEF. For (HCN)•••Li, the β_X and β_Z values change slightly when the AEF varies from 0.0004 to 0.0020 au and change sharply when the AEF is larger than 0.0020 au. For Li•••(HCN), the β_X and β_Z values do not have a sharp change until the AEF is larger than 0.0032 au (see Table 2).

Clearly, there is a plateau for the β_X and β_Z values of (HCN)•••Li and Li•••(HCN) clusters in an AEF range ~0.0004–0.0020 au with two basis sets. So, the computational results in this AEF range should represent the intrinsic properties of these species. Accordingly, AEF values in this plateau (e.g., 0.0010 au) are used in the following calculation for the electric properties.

The changes of the vertical ionization energies (VIEs) from 0.0000 to 0.0010 au AEF values are also rather small, 3.6% for (HCN)•••Li and 3.9% for Li•••(HCN). The change of the VIE values diminishes with the length of the HCN chain. Hereby, the 0.0010 au AEF is suitable in the calculations on the NLO properties of (HCN)_n•••Li and Li•••(HCN)_n (*n* = 1, 2, 3) clusters.

B. Basis Set Effects. The choice of suitable basis set to calculate the electric properties of the system which contains a loosely bound electron is important. For (HCN)•••Li and Li•••(HCN), effects of basis sets on calculations of the electric properties are studied at the MP2 level of theory with the 6-311++G(2d,2p), 6-311++G(2df,2p), 6-311++G(3df,3pd), and 6-311++G(3d2f,3pd) basis sets. The results are listed in Table 3. For the electric properties of (HCN)•••Li, in contrast to the smallest 6-311++G(2d,2p) values, the largest 6-311++G(3d2f,3pd) values only have slight changes, which are 0.4% for μ_0 , 1.2% for $\bar{\alpha}$, 1.3% for $|\Delta\alpha|$, and 6% for β_0 . For the electric properties of Li•••(HCN), the changes amount to 0.7%, 0.5%, 1.3%, and 11% for μ_0 , $\bar{\alpha}$, $|\Delta\alpha|$ and β_0 , respectively.

On the basis of the 6-311++G(3df,3pd) basis set, two sets of additional diffuse functions are added on the Li atom to study

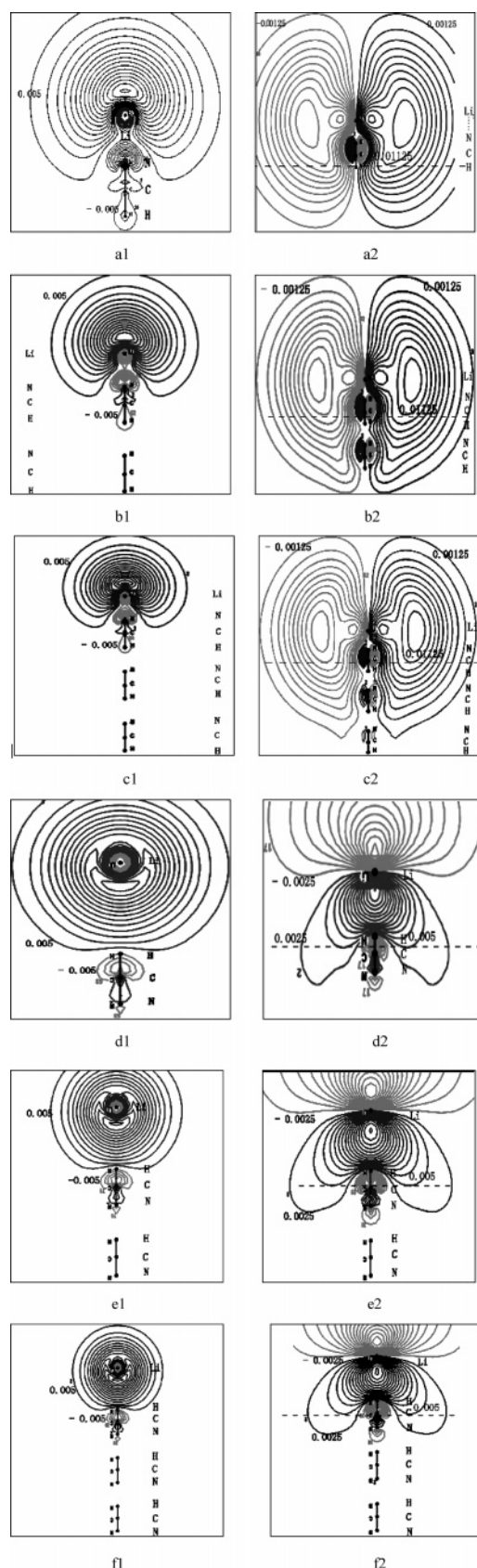


Figure 2. The HOMOs (left column) and vacant orbitals (right column) involved in the crucial excited states for (HCN)_n...Li (a, b, and c) and Li...HCN_n (n = 1, 2, 3) (d, e, and f). In a2, b2, and c2, dashed lines are the tangents to the 0.011 25 density contour line, moving from atom H to atom C with *n* = 1–3. In d2, e2, and f2, dashed lines are the tangents to the 0.005 density contour line, moving from the C–H bond to the C–N bond with *n* = 1–3.

TABLE 2: AEF Dependence of the β_x and β_z at MP2 Level of Theory with the 6-311++G(3df,3pd) and 6-311++G(3df,3pd)+D2 Basis Sets for (HCN)···Li and Li···(HCN)

fields (au)	(HCN)···Li				Li···(HCN)			
	basis set 1 ^a		basis set 2 ^b		basis set 1		basis set 2	
	β_x^c (au)	β_z (au)	β_x (au)	β_z (au)	β_x (au)	β_z (au)	β_x (au)	β_z (au)
0.0004	-50.3	-15693	-48.0	-14498	-6.2	-3370	-5.8	-3334
0.0008	-24.0	-15682	-33.6	-14571	-0.5	-3387	-1.6	-3341
0.0012	-45.2	-15733	-63.0	-14599	4.2	-3380	2.4	-3342
0.0016	-80.0	-15715	-114.6	-14639	7.8	-3369	3.6	-3334
0.0020	-124.2	-15695	-184.0	-14704	12.0	-3352	5.4	-3325
0.0024	-178.2	-15689	-2798.0	-19570	16.5	-3330	7.8	-3314
0.0028	-242.7	-15724	-57096	-3092	22.2	-3307	10.3	-3299
0.0032	-319.6	-15683	-42861	-4281	28.2	-3282	13.2	-3286
0.0040					42.6	-3222	-15710	-1632

^a 6-311++G(3df,3pd). ^b 6-311++G(3df,3pd)+D2 (D2 = 0.0037sp + 0.001 85sp + 0.000 925sp + 0.000 4625sp + 0.025d + 0.0125d + 0.006 25d). ^c $\beta_x = \frac{1}{3}(\beta_{xxz} + \beta_{xxx})$.

the effect of additional diffuse functions on the electric properties. These two sets of additional diffuse functions are denoted as D1 and D2 in the following discussion (D1 = 0.0037sp + 0.001 85sp + 0.000 925sp + 0.025d + 0.0125d (3s3p2d) and D2 = 0.0037sp + 0.001 85sp + 0.000 925sp + 0.000 4625sp + 0.025d + 0.0125d + 0.006 25d (4s4p3d)). The results are also listed in Table 3, which shows that the changes of the electric properties are quite small from the 6-311++G-(3df,3pd) to the 6-311++G(3df,3pd)+D2²⁵ basis sets. For (HCN)···Li, the change is 0.01% for μ_0 , 0.4% for $\bar{\alpha}$, and 6% for β_0 , and for Li···(HCN), the change is 0.019% for μ_0 , 0.05% for $\bar{\alpha}$, and 1% for β_0 . For the anisotropy $|\Delta\alpha|$, the 6-311++G-(3df,3pd)+D2 values are just 1% larger than the 6-311++G-(3df,3pd) values for the two models.

In brief, smooth convergences of the MP2 results are observed for μ_0 , $\bar{\alpha}$, $|\Delta\alpha|$, and β_0 in Table 3. The medium-sized 6-311++G(3df,3pd) basis set agrees well with the largest 6-311++G(3df,3pd)+D2 basis set for all calculated components of the NLO properties. It is obvious that, in this work, the effect of additional diffuse functions D2 on the NLO properties is negligible in 0.0010 au AEF. Thus, the 6-311++G(3df,3pd) basis set is suitable and employed in following discussions.

C. Electron Correlation Effects. Electron correlation effects calculated with the 6-311++G(3df,3pd) basis set are given in detail in Table 4. It is rather interesting to note that the MP2 method provides a theoretical description of the clusters' NLO properties quite close to those obtained with higher-order methods (e.g., QCISD, and so on).

For (HCN)···Li and Li···(HCN), different electron correlation effects are observed:

(1) For (HCN)···Li, the QCISD values are $\mu_0 = -3.104$ au, $\bar{\alpha} = 237.8$ au, $|\Delta\alpha| = 114.0$ au, and $\beta_0 = -15258$ au. In contrast to the HF values, electron correlation decreases the magnitude (about 8%) of μ_0 . For the anisotropy $|\Delta\alpha|$, the QCISD value is just 4% larger than the HF value. For α_{xx} , α_{zz} , and $\bar{\alpha}$, the electron correlation effects amount to 2%, 8%, and 3%, respectively. Very large electron correlation effects are observed for the β_0 value and two independent components (β_{xxz} and β_{zzz}), which are 27% for β_0 , 15% for β_{xxz} , and 175% for β_{zzz} . The QCISD β_0 value is close to the MP2 value and just 2% larger than the MP4(SDQ) and CCSD values.

(2) For Li···(HCN), the QCISD values are $\mu_0 = -1.643$ au, $\bar{\alpha} = 182.0$ au, $|\Delta\alpha| = 47.1$ au, and $\beta_0 = -3401$ au. In contrast to the HF values, electron correlation similarly decreases the magnitude of μ_0 (the change amounts to 6%). Slight changes are observed for the components of the dipole polarizability,

TABLE 3: Basis Set Effects on the Electric Properties of (HCN)···Li and Li···(HCN) System

properties (au)	6-311++G(2d,2p)	6-311++G(2df,2p)	6-311++G(3df,3pd)	6-311++G(3d2f,3pd)	6-311++G(3df,3pd) +D1 ^a	6-311++G(3df,3pd) +D2 ^b
(HCN)···Li						
μ_z	-3.116	-3.115	3.105	-3.105	-3.104	-3.104
α_{xx}	276.6	277.0	279.0	279.5	280.2	280.2
α_{zz}	156.3	156.9	157.9	158.2	158.3	158.3
$\bar{\alpha}$	236.5	237.0	238.6	239.1	239.6	239.6
$ \Delta\alpha $	120.3	120.1	121.1	121.3	121.9	121.9
β_{xxz}	-12401	-12373	-11312	-11414	-10676	-10677
β_{zzz}	-3427	-3530	-3615	-3640	-2959	-2959
β_0	-16936	-16964	-15682	-15879	-14585	-14587
Li···(HCN)						
μ_z	-1.619	-1.627	-1.626	-1.631	-1.626	-1.626
α_{xx}	165.0	164.9	166.5	166.6	166.6	166.6
α_{zz}	211.4	211.4	212.5	212.6	212.4	212.4
$\bar{\alpha}$	180.5	180.4	181.8	181.9	181.9	181.9
$ \Delta\alpha $	46.4	46.5	46.0	46.0	45.8	45.8
β_{xxz}	-1803	-1806	-1429	-1442	-1395	-1396
β_{zzz}	-2816	-2831	-2785	-2791	-2776	-2775
β_0	-3853	-3878	-3385	-3405	-3340	-3340

^a D1 = 0.0037sp + 0.001 85sp + 0.000 925sp + 0.025d + 0.0125d. ^b D2 = 0.0037sp + 0.001 85sp + 0.000 925sp + 0.000 4625sp + 0.025d + 0.0125d + 0.006 25d.

TABLE 4: Electron Correlation Effects on the Electric Properties of (HCN)···Li and Li···(HCN) System

properties (au)	HF	MP2	MP4(SDQ)	CCSD	QCISD
(HCN)···Li					
μ_z	-3.374	-3.105	-3.119	-3.105	-3.104
α_{xx}	269.9	279.0	276.0	275.3	275.8
α_{zz}	149.6	157.9	158.9	160.8	161.8
$\bar{\alpha}$	229.8	238.6	237.0	237.1	237.8
$ \Delta\alpha $	120.3	121.1	117.1	114.5	114.0
β_{xxz}	-9224	-11312	-10628	-10444	-10624
β_{zzz}	-1523	-3615	-3632	-3973	-4182
β_0	-11982	-15682	-14932	-14916	-15258
Li···(HCN)					
μ_z	-1.741	-1.627	-1.644	-1.641	-1.643
α_{xx}	166.2	166.5	166.2	166.3	166.3
α_{zz}	210.8	212.5	213.2	213.1	213.4
$\bar{\alpha}$	181.1	181.8	181.9	181.9	182
$ \Delta\alpha $	44.6	46.0	47.0	46.8	47.1
β_{xxz}	-1442	-1429	-1452	-1451	-1454
β_{zzz}	-3142	-2785	-2798	-2772	-2761
β_0	-3615	-3385	-3421	-3403	-3401

TABLE 5: Electron Properties of (HCN)_n···Li and Li···(HCN)_n ($n = 1, 2, 3$) at MP2/6-311++G(3df,3pd) Level

properties (au)	(HCN)···Li	(HCN) ₂ ···Li	(HCN) ₃ ···Li	Li···(HCN)	Li···(HCN) ₂	Li···(HCN) ₃
μ_z	-3.105	-4.847	-6.489	-1.626	-3.324	-4.995
α_{xx}	279.0	292.6	304.2	166.5	172.8	183.2
α_{zz}	157.9	191.4	220.5	212.5	243.8	273.3
$\bar{\alpha}$	238.6	258.9	276.3	181.8	196.5	213.2
$ \Delta\alpha $	121.1	101.2	83.7	46.0	71.0	90.0
β_{xxz}	-11312	-10456	-10192	-1429	-1857	-1969
β_{zzz}	-3615	-2684	-1489	-2785	-4265	-4741
β_0	-15682	-14159	-13119	-3385	-4790	-5206

0.06% for α_{xx} and 1.2% for α_{zz} . The QCISD mean $\bar{\alpha}$ and anisotropy $|\Delta\alpha|$ only increase by 0.5% and 5%, compared with HF values. More important changes are observed for β_{zzz} , and electron correlation decreases the value of β_{zzz} by 12%. For another component β_{xxz} , only a change of 0.6% is obtained. Overall, the total β_0 value decreases by 6%. For the first hyperpolarizability of the Li···(HCN) structure, we observe a smooth convergence in Table 4. The QCISD β_0 value is the same as the CCSD value and only 0.5% larger than the MP2 value.

Therefore, the MP2 method is suitable and employed in the following calculations of the NLO properties of (HCN)_n···Li and Li···(HCN)_n ($n = 1, 2, 3$).

3.3. NLO Properties of (HCN)_n···Li and Li···(HCN)_n Systems ($n = 1, 2, 3$). The NLO properties of (HCN)_n···Li and Li···(HCN)_n ($n = 1, 2, 3$) are calculated at the MP2/6-311++G(3df,3pd) level and listed in Table 5. The contribution of the Li atom to the polarizability and first hyperpolarizability of investigated systems is also calculated at the MP2/6-311++G(3df,3pd) level with the CP method. The data are displayed in Table 6. Three rules are observed from Tables 5 and 6: (1) The polarizabilities and first hyperpolarizabilities of such new clusters are large, compared with some traditional NLO matters (see Introduction). Such large values are dominated by the Li atom. (2) The first hyperpolarizabilities of (HCN)_n···Li are larger than those of Li···(HCN)_n ($n = 1, 2, 3$).

TABLE 6: Alkali Metal Contribution to the Polarizabilities and First Hyperpolarizabilities of (HCN)_n...Li and Li... (HCN)_n (n = 1, 2, 3) at MP2/6-311++G(3df,3pd) Level

system	$\bar{\alpha}$				β_0			
	ALi	A ^a	ALi-A	(ALi-A)/ALi	ALi	A	ALi-A	(ALi-A)/ALi
(HCN)...Li	238.6	16.4	222.2	93.13%	-15682	4.2	-15677	99.96%
(HCN) ₂ ...Li	258.9	33.7	225.2	86.98%	-14159	-25.9	-14133	99.81%
(HCN) ₃ ...Li	276.3	51.6	224.7	81.32%	-13119	-61.7	-13057	99.53%
Li... (HCN)	181.8	16.4	165.4	90.98%	-3878	-2.9	-3875	99.92%
Li... (HCN) ₂	196.5	33.7	162.8	82.85%	-4790	-27.0	-4763	99.44%
Li... (HCN) ₃	213.2	51.5	161.7	75.84%	-5206	-63.4	-5147	98.87%

^a A stands for the (HCN)_n cluster (n = 1, 2, and 3).

TABLE 7: The Crucial Excited State of (HCN)_n...Li and Li... (HCN)_n (n = 1, 2, and 3) by CIS Method^a

	(HCN) _n ...Li			Li... (HCN) _n		
	n = 1	n = 2	n = 3	n = 1	n = 2	n = 3
ΔE (eV)	1.3311	1.3566	1.3636	1.8165	1.8246	1.8306
f_0	0.1886	0.2044	0.2086	0.2639	0.2659	0.2666
λ	931	914	909	682	679	677
transition orbital of	HOMO →	HOMO →	HOMO →	HOMO →	HOMO →	HOMO →
crucial excited state	LUMO + 1	LUMO + 1	LUMO + 2	LUMO	LUMO	LUMO
nature	$\sigma \rightarrow \pi^*$	$\sigma \rightarrow \pi^*$	$\sigma \rightarrow \pi^*$	$\sigma \rightarrow \sigma^*$	$\sigma \rightarrow \sigma^*$	$\sigma \rightarrow \sigma^*$
β_0 (au)	-15682	-14159	-13119	-3385	-4790	-5206

^a ΔE is the transition energy and f_0 is the oscillator strength. 1 au = 9.6392×10^{-33} esu.

(3) For the (HCN)_n...Li (n = 1, 2, 3) system, the absolute values of the first hyperpolarizabilities decrease with the length of the HCN chain for n = 1–3 ($\beta_0 = -15\,682$ au for n = 1, $\beta_0 = -14\,159$ au for n = 2, and $\beta_0 = -13\,119$ au for n = 3). Oppositely, for the Li... (HCN)_n (n = 1, 2, 3) system, the absolute values of the first hyperpolarizabilities increase with the length of the HCN chain ($\beta_0 = -3385$ au for n = 1, $\beta_0 = -4790$ au for n = 2, and $\beta_0 = -5206$ au for n = 3).

A. Contribution of Alkali Metal. Our final values for metal contributions are obtained as ALi – A (see eqs 6–7) in Table 6 (A stands for the (HCN)_n part). Table 6 shows that the dominant contribution to the β_0 values derives from the Li atom and amounts to more than 98% of the total β_0 value. However, it is well-known that the β_0 value of the Li atom itself is close to naught, normally. Only under the action of the (HCN)_n cluster is the valence electron of the Li atom ejected from the 2s orbital to be an excess electron, which may bring the large β_0 values for (HCN)_n...Li and Li... (HCN)_n. In addition, because of the effect of the ghost orbitals of the Li atom in the CP calculation, the first hyperpolarizability of the HCN moiety in (HCN)_n...Li or Li... (HCN)_n is slightly different from that of the monomer.²⁶

Owing to the complexity of the sum-over-states (SOS) expression, Oudar and Chemala^{27,28} established a link between β and the details of a low-lying charge-transfer transition through the two-level model. The static case ($\omega = 0.0$) is assumed, and the following two-level expression is found to calculate β_0 in the literature:^{19,28}

$$\beta_0 = (3/2)\Delta\mu \cdot f_0 / \Delta E^3 \quad (8)$$

where ΔE , f_0 , and $\Delta\mu$ are the transition energy, oscillator strength, and the difference of dipole moment between the ground state and the crucial excited state, respectively.

Single excitation configuration interaction (CIS) calculations are carried out to get the crucial excited state of the two classes of clusters. The CIS results are listed in Table 7. The data show that there is a primary HOMO → LUMO + 1 transition for n = 1 and 2 or a primary HOMO → LUMO + 2 transition for n = 3 in the (HCN)_n...Li system. For Li... (HCN)_n, the transition between the ground state and the crucial excited state is corresponding to HOMO → LUMO transition. The HOMOs

and virtual orbitals involved in the crucial transitions are pictured in Figure 2. From Figure 2, it is very clear that the transitions between the ground state and the crucial excited state are assigned as $\sigma \rightarrow \pi^*$ transitions for (HCN)_n...Li (n = 1, 2, 3) and $\sigma \rightarrow \sigma^*$ transitions for Li... (HCN)_n (n = 1, 2, 3). Obviously, each orbital involved in the two-state expression is principally composed of metal Li orbitals for (HCN)_n...Li and Li... (HCN)_n. It explains that such large first hyperpolarizabilities of (HCN)_n...Li and Li... (HCN)_n are dominated by the Li atoms.

B. Differences between Two Models. Linear (HCN)_n clusters possess two oppositely directed polar terminals. The terminal N atom is an electron-pushing group, and the terminal H atom is an electron-pulling group. The Li atom is a highly polarizable system.²⁹ When the Li atom interacts with the terminal N atom, the 2s electron of the Li atom is pushed out by the lone pair of the N atom, and the Li atom becomes an electron acceptor (Figure 1a and Figure 2a1, 2b1, 2c1). When the Li atom interacts with the terminal H atom, the 2s electron of the Li atom is pulled to the H atom, and the Li atom becomes an electron donor (Figure 1b and Figure 2d1, 2e1, 2f1). It shows that the interaction between the Li atom and the (HCN)_n cluster in (HCN)_n...Li differs from that in Li... (HCN)_n.

Obviously, the Li atom ionizes and resembles Li⁺ with a Rydberg-like excess electron in two classes of clusters. As shown in Figure 2 (the HOMO plots), the Li atom has a big diffuse orbital, and its valence electron is loosely bound in clusters. As a result, these clusters have very low-lying excited states, requiring lower transition energy in crucial transition (as shown in Table 7 and Table 8). So, (HCN)_n...Li and Li... (HCN)_n have the large first hyperpolarizabilities naturally.

However, why are the first hyperpolarizabilities of (HCN)_n...Li far larger than those of Li... (HCN)_n (n = 1, 2, 3)? According to the two-level expression, the β_0 value is inversely proportional to the third power of the transition energy. From Table 7, we find that the transition energies of (HCN)_n...Li are smaller than those of Li... (HCN)_n. Therefore, the β_0 values of (HCN)_n...Li are larger than those of Li... (HCN)_n.

Another important influencing factor is the charge transfer in crucial transition.^{30,31} In this paper, the charge transfers from the Li atom to the (HCN)_n cluster in crucial transitions for two classes of clusters. (HCN)_n...Li and Li... (HCN)_n are two ex-

TABLE 8: Calculated Excited States by the SAC–CI Method for (HCN)•••Li and Li•••(HCN)

(HCN)•••Li			Li•••(HCN)		
symmetry	ΔE (eV)	f_0	symmetry	ΔE (eV)	f_0
1 ² A ₁	0.0		1 ² A ₁	0.0	
1 ² B ₂	1.6452	0.2439	2 ² A ₁	1.8311	0.2757
1 ² B ₁	1.6548	0.2460	1 ² B ₁	1.9222	0.2515
2 ² A ₁	1.7529	0.0291	1 ² B ₂	1.9222	0.2515
2 ² B ₁	2.6956	0.0206	2 ² B ₁	4.0621	0.0009
2 ² B ₂	2.7183	0.0174	2 ² B ₂	4.0621	0.0009
3 ² B ₂	3.3098	0.0039	3 ² B ₂	4.5083	0.0002
1 ² A ₂	4.2348	0.0000	1 ² A ₂	5.0404	0.0000

amples to analyze the effect of the charge transfer. For (HCN)•••Li, the HOMO presents a misshapen s character. The excess electron distribution in the surface structure is localized near the Li atom at the opposite side of the HCN molecule (Figure 2a1). The LUMO + 1 is a misshapen p character, which extends to HCN and almost encases the HCN molecule (Figure 2a2). For Li•••(HCN), the HOMO with s character is localized between the Li atom and the H atom. And, the LUMO with p character has a further extension toward the HCN molecule in the same directions (Figure 2d1 and 2d2). Observing two charge-transfer modes, the reverse-direction charge-transfer from $\sigma \rightarrow \pi^*$ transition in (HCN)•••Li is larger than the same-direction charge-transfer from $\sigma \rightarrow \sigma^*$ transition in Li•••(HCN). The large charge transfer can bring the large contribution to the first hyperpolarizability. It is another important reason that the first hyperpolarizabilities of (HCN)_n•••Li are much larger than those of Li•••(HCN)_n ($n = 1, 2, 3$).

To confirm the CIS results, the symmetry-adapted cluster-configuration interaction (SAC-CI) method is employed to calculate the excited states of (HCN)•••Li and Li•••(HCN). Data are given in Table 8. (HCN)•••Li and Li•••(HCN) are linear structures with $C_{\infty v}$ symmetry, of which the largest abelian group is C_{2v} in the calculation. In Table 8, for (HCN)•••Li, the crucial transition is assigned as 1 ²A₁ \rightarrow 1 ²B₂ and 1 ²A₁ \rightarrow 1 ²B₁ (degenerate states) with oscillator strengths of 0.2439 and 0.2460, respectively. Their transition energies are 1.6452 and 1.6548 eV, which are only 0.3 eV larger than the CIS result (1.3311 eV). When C_{2v} symmetry is reverted to $C_{\infty v}$ symmetry, the nature of the 1 ²A₁ state is assigned as σ character, and the nature of 1 ²B₂ + 1 ²B₁ state is assigned as π^* character. As a result, the crucial transition of (HCN)•••Li is still confirmed as a $\sigma \rightarrow \pi^*$ transition by the SAC-CI method. For Li•••(HCN), the SAC-CI result shows that the crucial transition is 1 ²A₁ \rightarrow 2 ²A₁, which is a $\sigma \rightarrow \sigma^*$ transition. Its transition energy is 1.8311 eV, quite close to the CIS result (1.8165 eV).

In brief, the SAC-CI results show that (a) the transition energies of two species are comparatively small (1.6452 or 1.6548 eV for (HCN)•••Li and 1.8311 eV for Li•••(HCN)), (b) the transition energy of (HCN)•••Li is smaller than that of Li•••(HCN), and (c) the transition types of the crucial transitions are $\sigma \rightarrow \pi^*$ for (HCN)•••Li and $\sigma \rightarrow \sigma^*$ for Li•••(HCN). These conclusions prove that the CIS results are reliable in this paper.

C. The n -Dependence of the First Hyperpolarizability. Our findings for the relationship between the β_0 value and the number n of the (HCN)_n clusters are given in Table 5. For (HCN)_n•••Li ($n = 1, 2, 3$), from $n = 1$ to $n = 3$, the absolute values of the first hyperpolarizability decrease. Oppositely, for Li•••(HCN)_n ($n = 1, 2, 3$), the absolute values of the first hyperpolarizability increase with the length of the HCN chain. In each class of clusters, as the differences of the transition energies are very small, the charge transfer in the crucial transition is a main factor in the different first hyperpolarizability.

For (HCN)_n•••Li ($n = 1, 2, 3$), comparisons of Figure 2a–c show that the shapes of the HOMOs are almost the same, but the shapes of unoccupied molecular orbitals (LUMO + 1 or LUMO + 2) are obviously different. These unoccupied orbitals may be related to the n -dependence. To clarify this phenomenon, dashed lines are appended in the contour plots of the unoccupied molecular orbitals (Figure 2a2, 2b2, and 2c2), which are the tangents to the 0.011 25 density contour line. With the neighboring HCN molecule as a marker, we find that the dashed lines cross the C–H bond of the neighboring HCN molecule, and the crossings move gradually from the H atom to the C atom from $n = 1$ –3. Clearly, in LUMO + 1 or LUMO + 2, the p-character orbital from the Li atom encases the neighboring HCN molecule, but the extent decreases with the length of the HCN chain. It implies that the intermolecular charge transfer in the crucial transitions is weakened step by step with the length of the HCN chain. As a result, a rule occurs that the $|\beta_0|$ values of (HCN)_n•••Li system decrease with the length of the HCN chain.

Similarly, for Li•••(HCN)_n ($n = 1, 2, 3$), comparisons of Figure 2d–f show that the shapes of the HOMOs are like each other, but the shapes of the LUMOs are different. In the LUMOs, the tangents to the 0.005 density contour line are appended and cross the neighboring HCN molecule (Figure 2d2, 2e2, and 2f2). The crossings move step by step from the C–H bond to the C–N bond from $n = 1$ –3. Clearly, the extent of the same density contour line encasing HCN increases with the length of the HCN chain. It implies that the intermolecular charge transfer is strengthened step by step in the crucial transitions with the length of the HCN chain. Therefore, another rule occurs that the $|\beta_0|$ values of Li•••(HCN)_n increase with lengthening of the HCN chain.

In the present work, we have obtained a complete description of the first hyperpolarizabilities of (HCN)_n•••Li and Li•••(HCN)_n ($n = 1, 2, 3$). It indicates that these new alkali metal–molecule clusters have large nonlinear optical responses. In these species, alkali metal atoms ionize to form cations and excess electrons under the action of the (HCN)_n clusters. Thus, these clusters have very low-lying excited states to bring such large β_0 values. Obviously, such large values are dominated by the Li atom. This structural characteristic (alkali cations + excess electrons) is highly similar to the electrified structure model in nature. As a result, our investigation of the large first hyperpolarizabilities of (HCN)_n•••Li and Li•••(HCN)_n ($n = 1, 2, 3$) may evokes one's attention to unusual NLO responses of some electrides and encourage one to study them.

Acknowledgment. This work was supported by the National Natural Science Foundation of China (no. 20273024) and the Innovation Fund of Jilin University.

References and Notes

- (1) Eaton, D. F. *Science* **1991**, 253, 281.
- (2) *Nonlinear Optical Properties of Organic Molecules and Polymeric Materials*; Williams, D. J., Ed.; ACS Symposium Series 233; American Chemical Society: Washington, DC, 1984.
- (3) Cheng, W. D.; Xiang, K. H.; Pandey, R.; Pernisz, U. C. *J. Phys. Chem. B* **2000**, 104, 6737.
- (4) Ichida, M.; Sohda, T.; Nakamura, A. *J. Phys. Chem. B* **2000**, 104, 7082.
- (5) Hold, K.; Pawlowski, F.; Jørgensen, P.; Hättig, C. *J. Chem. Phys.* **2003**, 118, 1292.
- (6) Hättig, C.; Larsen, H.; Olsen, J.; Jørgensen, P.; Koch, H.; Fernández, B.; Rizzo, A. *J. Chem. Phys.* **1999**, 111, 10099.
- (7) Horikoshi, R.; Nambu, C.; Mochida, T. *Inorg. Chem.* **2003**, 42, 6868.
- (8) Long, N. J.; Williams, C. K. *Angew. Chem., Int. Ed.* **2003**, 42, 2586.
- (9) Shelton, D. P.; Rice, J. E. *Chem. Rev.* **1994**, 94, 3.

- (10) Li, Y.; Li, Z. R.; Wu, D.; Li, R. Y.; Hao, X. Y.; Sun, C. C. *J. Phys. Chem. B* **2004**, *108*, 3145.
- (11) Dye, J. L. *Inorg. Chem.* **1997**, *36*, 3816.
- (12) Ichimura, A. S.; Dye, J. L. *J. Am. Chem. Soc.* **2002**, *124*, 1170.
- (13) (a) Dye, J. L. *Science* **2003**, *301*, 607. (b) Matsuishi, S. *Science* **2003**, *301*, 626.
- (14) Dye, J. L.; Echegoyen, L.; Kiefer, A. *Physical Supramolecular Chemistry*; Kluwer Academic Publishers: Dordrecht, Netherlands, 1996; p 313.
- (15) Hendrickson, J. E.; Pratt, W. P., Jr.; Kuo, C.-T.; Xie, Q.; Dye, J. L. *J. Phys. Chem.* **1996**, *100*, 3395.
- (16) Iwata, S.; Tsurusawa, T. In *Advances in Metal and Semiconductor Clusters*; JAI Press: Greenwich, CN, 2001; Vol. 5, pp 39–75.
- (17) Gutowski, M.; Skurski, P. *Chem. Phys. Lett.* **1999**, *300*, 331.
- (18) Klahn, Th.; Krebs, P. *J. Chem. Phys.* **1998**, *109*, 543.
- (19) Kanls, D. R.; Ratner, M. A.; Marks, T. J. *Chem. Rev.* **1994**, *94*, 195.
- (20) Petkov, V.; Billinge, S. J. L.; Vogt, T.; Ichimura, A. S.; Dye, J. L. *Phys. Rev. Lett.* **2002**, *89*, 075502.
- (21) Li, Z. Y.; Yong, J. L.; Hou, J. G.; Zhu, Q. S. *J. Am. Chem. Soc.* **2003**, *125*, 6050.
- (22) Buckingham, A. D. *Adv. Chem. Phys.* **1967**, *12*, 107. Mclean, A. D.; Yoshimine, M. *J. Chem. Phys.* **1967**, *47*, 1927.
- (23) Boys, S. F.; Bernardi, F. *Mol. Phys.* **1970**, *19*, 553.
- (24) Frisch, M. J.; Trucks, G. W.; Schlegel, H. B.; Scuseria, G. E.; Robb, M. A.; Cheeseman, J. R.; Montgomery, J. A., Jr.; Vreven, T.; Kudin, K. N.; Burant, J. C.; Millam, J. M.; Iyengar, S. S.; Tomasi, J.; Barone, V.; Mennucci, B.; Cossi, M.; Scalmani, G.; Rega, N.; Petersson, G. A.; Nakatsuji, H.; Hada, M.; Ehara, M.; Toyota, K.; Fukuda, R.; Hasegawa, J.; Ishida, M.; Nakajima, T.; Honda, Y.; Kitao, O.; Nakai, H.; Klene, M.; Li, X.; Knox, J. E.; Hratchian, H. P.; Cross, J. B.; Adamo, C.; Jaramillo, J.; Gomperts, R.; Stratmann, R. E.; Yazyev, O.; Austin, A. J.; Cammi, R.; Pomelli, C.; Ochterski, J. W.; Ayala, P. Y.; Morokuma, K.; Voth, G. A.; Salvador, P.; Dannenberg, J. J.; Zakrzewski, V. G.; Dapprich, S.; Daniels, A. D.; Strain, M. C.; Farkas, O.; Malick, D. K.; Rabuck, A. D.; Raghavachari, K.; Foresman, J. B.; Ortiz, J. V.; Cui, Q.; Baboul, A. G.; Clifford, S.; Cioslowski, J.; Stefanov, B. B.; Liu, G.; Liashenko, A.; Piskorz, P.; Komaromi, I.; Martin, R. L.; Fox, D. J.; Keith, T.; Al-Laham, M. A.; Peng, C. Y.; Nanayakkara, A.; Challacombe, M.; Gill, P. M. W.; Johnson, B.; Chen, W.; Wong, M. W.; Gonzalez, C.; Pople, J. A. *Gaussian 03*, revision B.03; Gaussian, Inc.: Pittsburgh, PA, 2003.
- (25) The geometry parameters of (HCN)···Li and Li···(HCN) are calculated with the 6-311++G(3df,3pd)+D2 basis set. Except for the H–Li distance of Li···(HCN), changes of other parameters are small ($r = 1.0670$ au, $R = 1.1601$ au, and $L = 2.0878$ au for (HCN)···Li; and $r = 1.0665$ au, $R = 1.1657$ au, and $L = 4.0037$ au for Li···(HCN)). The HOMOs obtained with 6-311++G(3df,3pd)+D2 and 6-311++G(2df,2p) basis sets are almost the same.
- (26) Maroulis, G. *Chem. Phys. Lett.* **2001**, *334*, 207.
- (27) Oudar, J. L.; Chemla, D. S. *J. Chem. Phys.* **1977**, *66*, 2664.
- (28) Oudar, J. L. *J. Chem. Phys.* **1977**, *67*, 446.
- (29) Politzer, P.; Jin, P.; Murray, J. S. *J. Chem. Phys.* **2002**, *117*, 8197.
- (30) Zyss, J.; Nicoud, J. F.; Coquillay, M. *J. Chem. Phys.* **1984**, *81*, 4160.
- (31) Cassidy, C.; Halbout, J. M.; Donaldson, W.; Tang, C. L. *Opt. Commun.* **1979**, *29*, 243.